ARTICLES

Mechanisms of Nonexponential Relaxation in Supercooled Glucose Solutions: the Role of Water Facilitation

Valeria Molinero,[†] **Tahir Çağın,**[‡] **and William A. Goddard, III***

Materials and Process Simulation Center, California Institute of Technology (MC 139-74), Pasadena, California 91125

Concentrated sugar solutions are prototypical glass formers with a wide application in food technology and cyropreservation, but the microscopic mechanisms underlying these processes remain obscure. To uncover these microscopic details, we study the structure and dynamics of binary glucose−water mixtures by means of atomistic and coarse grain molecular dynamics simulations. From atomistic simulations, we find that water in glucose forms extended clusters that percolate above a water concentration of ∼18 wt % at $T = 340$ K. This percolation threshold and structure is very well reproduced with a coarse grain model even though it lacks of directional interactions. Using the coarse grain model, we present a detailed study of the translational dynamics of the 12.2 wt % water mixture in the temperature range $T/T_g = 1.5−1.05$ and for times up to 0.65 μs. These coarse grain studies lead to a glass transition temperature of 239 ± 25 K in excellent agreement with the experimental value of 240 K. The water diffusion coefficient obtained from these calculations has an activation energy of 35−38 kJ/mol, which compares very well with the 31 kJ/mol obtained experimentally for the 25 wt % water−glucose mixture. Both water and glucose show nonexponential relaxation, although the nonexponentiallity is more pronounced for water. We find that water diffusion in supercooled glucose proceeds by two mechanisms: (i) continuous diffusion and (ii) discrete jumps on the order of 3 Å. The contribution of the jump mechanism increases with supercooling. On the other hand, the continuous diffusion component of water diffusion decreases at lower temperatures until it becomes negligible for $T < 1.2T_g$. At this point rare jump events with characteristic times above 10 ns are the only mechanism of water relaxation. The decrease of the extent of the continuous diffusion to water mobility with lowering temperatures is associated with the freezing of the sugar matrix. In the deep supercooled regime, at $T/T_g = 1.05$ water moves in an almost translationally frozen glucose matrix, and displays a broad distribution of waiting times between jumps. Contrary to water, the mechanism of glucose translation does not involve big jumps even at the lowest temperatures analyzed. Rather the center of mass of the glucose molecules translate through a continuous diffusion mechanism with a distribution of characteristic times. We analyze the mobility of water molecules as a function of the water−water connectivity and find that the mobility of the water molecules increases with their water coordination. The lower the temperature the more important the effect of water coordination in water mobility. The distribution of mobilities associated with different water local environments constitutes a structural contribution to the heterogeneous, nonexponential dynamics in the binary mixture.

1. Introduction

It is known that formation of glasses plays a role in preventing chemical and textural degradation of the foods.[1] However, recent studies of carbohydrate solutions found that water can still diffuse in the glassy carbohydrate matrices, proving that vitrification is not a sufficient condition to arrest water mobility:[2−4] These findings have important practical effects on the chemical stability of glassy carbohydrate−water mixtures,[5,6] with potential strong economical impact through the shelf life of food, pharmaceutical, and cryopreserved products. To

understand the nature of water diffusion in glassy foodlike systems, we have examined low water content glucose mixtures, a simple binary glass-former that is considered to be a model for food systems.[1]

There is no direct evidence for the microscopic mechanism of water diffusion in supercooled concentrated carbohydrate solutions. Magazú et al.[7] reported two distinct mechanisms for water and trehalose from the analysis of neutron scattering experiments of 54 wt % water in trehalose at 309 K:

(i) A continuous diffusion mechanism for the translation of the sugar.

(ii) A jump-diffusion mechanism for the water molecules.

Using the same technique, Feeney et al.[8] studied water mobility in fructose with 40, 71, and 96 wt % water at 300 K and found results consistent with a transition from continuous

* To whom correspondence should be addressed. E-mail: wag@caltech.edu. Telephone: 1-626-395-2731. Fax: 1-626- 585-0918.
† E-mail: vale@wag.caltech.edu.
‡ E-mail: tahir@wag.caltech.edu.

to jump-diffusion mechanism between 71 and 96 wt % water. These later authors also interpreted water relaxation in terms of a stretched exponential decay and found a significant nonexponential behavior only for the lowest water content solution.[8]

Using deuterium NMR studies of the diffusivity of water and glucose in 25 wt % and 60 wt % water in glucose, Moran et al.[9] showed that the relaxation for water is highly nonexponential, while the sugar relaxation can be represented by a single characteristic time. They observed that in the supercooled regime both water and glucose diffusion coefficients have Arrhenius temperature dependence. They found that for 60 wt % water these two diffusion coefficients have similar activation energies (E_a), but for the concentrated 25 wt % solution the E_a for glucose is almost twice that of water.[9] The same decoupling of a probe dynamics and the viscosity of the solution was found for sucrose with water concentrations below 40 wt %[10] In a recent publication,[11] we showed that the onset of decoupling in water–sucrose solutions coincides with the formation of a three-dimensional hydrogen bonded network between the saccharide molecules.

In an NMR study of the mobilility in maltose glasses with 5–20 wt % water, Van den Dries et al.[4] showed that below the glass transition temperature (T_g) water mobility continues to be detected, but the number of protons corresponding to the mobile fraction is lower than the total of the water molecules. They also found that for water contents of 5–10 wt % the strength of the dipolar interactions shows a considerable change in slope at T_g. However, for 20 wt % water content, the change in the strength of the dipolar interactions with temperature is nearly insensitive to the glass transition temperature. This result suggests that there may be a structural contribution from the water distribution that allows a relaxation pathway in a frozen sugar matrix, which would explain why water diffusion is so sensitive to the dynamics of the matrix at low water content and is almost independent of it for the highest water content.

Dielectric relaxation studies of water–maltose mixtures[12] also showed a significant change in the relative strength of the dipolar relaxation with water content: the loss ϵ'' of the secondary peak (β relaxation) at 213 K changes slowly with water content from 0 to 11.5 wt % water, and its intensity doubles between 11.5 and 15 wt % water and then continues to increase with water content. These authors claim that this change in slope of ϵ'' vs wt % is absent in glucose–water mixtures, but they studied mixtures with water content 0, 5, and 12 wt % whereas the change in slope would be expected at a slightly higher water content.

In our previous atomistic simulations of the structure of water–sucrose solutions,[11] we found that water has a locally heterogeneous structure (in agreement simulations of other water–carbohydrate solutions[13]) with a percolation threshold between 10 and 18 wt % water content. We showed that the free volume in water–sucrose mixtures is nonmonotonic with increasing water content and that the percolation of the free volume pathways occurs for a probe radius much smaller than the water size. These results reinforce the idea that water diffusion in supercooled and frozen matrices is not determined by the free-volume but rather it might be strongly coupled to the water structure. In a frozen matrix with low water content, we would expect the water pathways to facilitate water diffusion.

Understanding and predicting water diffusivity in supercooled and glassy carbohydrates is of utmost importance in the practical applications of these mixtures but is even more interesting from a fundamental point of view is the elucidation of the differential

microscopic processes that allow the diffusion of a small component below the glass transition of the mixture.[14] This should allow us to understand the origin of the different relaxations in supercooled and glassy binary mixtures. The aim of the present work is to provide a microscopic analysis of the structure and dynamics of concentrated glucose solutions close to the glass transition, from $T/T_g = 1.5$ to 1.04. We present a molecular dynamics study of the distribution of water in concentrated glucose mixtures (8–20 wt % water) and the characterization of the mechanisms of water and glucose translational diffusion in moderately supercooled and deep supercooled regime.

Section 2 describes the methodology while section 3 discusses the results on the structure and dynamics. Section 4 summarizes the results, and section 5 provides the conclusions.

2. Methods for Molecular Dynamics Simulations

Constant volume and constant pressure atomistic molecular dynamics (MD)[15] simulations were performed using Cerius2.[16] The integration of the equations of motion was done with the Verlet Leap-Frog algorithm,[15] using a time step of 0.001 ps. The MD was performed in the isothermal–isobaric ensemble (NPT), except when indicated otherwise. The temperature was controlled with a Nose–Hoover thermostat[17] using a time constant $\tau = 50$ times the MD time step. The pressure was controlled with the Rahman–Parrinello algorithm[18] with a fictitious mass of the cell coordinates of $W = 0.2$ times the mass of the particles in the cell.

2.1. Atomistic Simulations. Water and glucose were modeled as all-atom fully flexible molecules using the DREIDING force field[19] energy expression that consists of a sum of valence interactions between connected atoms (two body harmonic bonds, three body cosine harmonic angle term, and four body dihedral torsion angle terms) plus two nonbonded interactions (two body exponential–six van der Waals terms and coulomb interactions between partial charges on the atoms, and three body hydrogen bond term). The atom type assignment and their respective parameters were those of the DREIDING force field.[19] Geometric combination rules for the van der Waals interactions between different atom types, except that we defined explicit off-diagonal exponential-6 van der Waals interactions between any carbohydrate oxygen and the hydroxylic hydrogen atoms with the parameters $D = 0.03783$ kcal/mol, $R = 2.4$ Å, and $\xi = 12.76$, instead of using the geometric combination rule. The hydrogen bond parameters were taken as $D_{OO} = 2.5$ kcal/mol and $R_{OO} = 3.2$ Å. Partial charges on carbohydrate atoms were obtained by charge equilibration [20] in a water box with density 1 g/cm^3 and $T = 300$ K, averaged over a 10 ps *NVT* simulation. Partial charges on water molecule were obtained by LMP2 quantum mechanics calculations, leading to $q_O = -2q_H = -0.7287$ eu. Long-range interactions in the periodic systems were evaluated with Ewald sums.[21] The modification of the cross interactions between the sugar's hydroxyl groups was based on fitting crystal structure and amorphous data to improve the matching between the experimental and simulated density for glucose, sucrose and fructose. The densities obtained with the modified Dreiding force field at 300 K and 1 atm are as follows:

(I) 1.48 ± 0.02 g/cm^3 for amorphous α-D-glucose,[22] which compares well with the experimental 1.52 g/cm^3.[23]

(II) 1.56 ± 0.01 g/cm^3 for crystalline α-D-glucose,[24] which compares well with the experimental 1.566 g/cm^3.[23]

(III) 1.46 ± 0.02 g/cm^3 for amorphous sucrose,[11] which compares well with the experimental 1.43 g/cm^3.[25]

Mechanisms of Relaxation in Water−Glucose

J. Phys. Chem. A, Vol. 108, No. 17, 2004 **3701**

TABLE 1: Composition and Density of Water−Glucose Mixtures

wt % water	no. of waters	no. of glucoses	$\rho_{atom}{}^a$	$\rho_{M3B}{}^b$
8.0	35	40	1.415 ± 0.010	1.379 ± 0.003
12.2^c	56	40	1.397 ± 0.011	1.358 ± 0.003
16.5	79	40	1.381 ± 0.006	1.335 ± 0.003
20.0	100	40	1.373 ± 0.005	1.315 ± 0.003

^{a} $T = 343 \pm 8$ K. Each density was averaged over the last 20 ps for 4 independently built cells. ^{b} $T = 338 \pm 18$ K. Each density was averaged over the last 1 ns for 5 independently built cells. ^{c} A larger system with 90 glucose and 125 water molecules was prepared for the study of the dynamics and glass transition using the M3B coarse grain model.
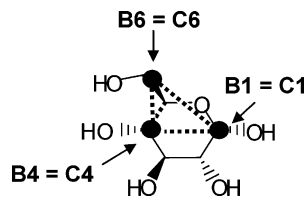
Figure 1. M3B coarse grain model of glucose molecule superimposed on the atomistic description. The positions of the M3B particles correspond to those of the carbon atoms C1, C4, and C6 of α-glucose.

(IV) 1.594 ± 0.002 g/cm³ for crystalline sucrose,[11] which compares well with the experimental 1.59 g/cm³.[26]

(V) 1.59 ± 0.01 g/cm³ for crystalline β-D-fructopyranose,[24] which compares well with the experimental 1.60 g/cm³.[27]

(VI) The densities of water−sucrose *mixtures* are predicted within 2% of the experimental value, in all concentration ranges.[11]

We prepared concentrated glucose−water amorphous mixtures with water content in the range 8−20 wt % The number of α-D-glucose and water molecules per cell is listed in Table 1.We have not found experimental densities of water−glucose solutions in this concentration range. For each composition, a set of four independent equilibrated amorphous atomistic samples were prepared and equilibrated at $T = 343$ K and $p = 1$ atm following the CED procedure,[28] which involves a series of compression/expansion and annealing steps, designed to fully equilibrate the structure of amorphous systems built through Monte Carlo techniques. The structure of the mixtures was analyzed over the last 20 ps of each equilibration trajectory.

2.2. Coarse Grain Simulations. The coarse grain simulations were performed with the M3B model and force field.[22] This force field was parametrized from atomistic simulations of amorphous glucose and maltooligosaccharides, using the same atomistic force field used in this work. M3B predicts the density for pure amorphous glucose within 2% of the atomistic value in the pressure range −2 to 20 GPa.[22] The M3B model represents each glucose molecule by three particles (beads) connected through bonds. The M3B model is mapped from the atomistic glucose, placing the three beads in the positions of carbons C1, C4, and C6, as shown in Figure 1. The intramolecular interactions of glucose are completely defined by three harmonic bonds between the beads. The parameters of the bond interactions are shown in Table 2. The intermolecular interactions between glucose molecules are described by the sum of Morse nonbond interaction among all pairs of beads of the different molecules,

$$V(R_{ij}) = D_o\{(e^{-0.5\alpha(R_{ij}/R_o-1)})^2 - 2(e^{-0.5\alpha(R_{ij}/R_o-1)})\} \quad (1)$$

where R_o is the distance for the minimum energy (D_o) and α is

TABLE 2: M3B Bond Parameters. $E(r) = {}^1\!/_2 k(r - r_o)^2$

bond type^a	r_o (Å)	K, (kcal mol^{-1} Å^{-2})
14	2.93	425
16	3.69	235
46	2.60	435

^{a} The bond type ij corresponds to the bond between bead B$_i$ and B$_j$ (numbered as in Figure 1).

TABLE 3: M3B Masses and Morse Parameters for Glucose and Water Beads

bead	mass (amu)	R_o (Å)	D_o (kcal mol^{-1})	α
B1	75	5.13	2.05	11
B4	75	6.11	1.95	10.5
B6	30	4.63	1.79	11
W	18	3.77	1.15	8

a measure of the curvature of the potential around R_o. In the coarse grain model the water molecule is represented by a single bead (W) that interacts with glucose and other water molecules through a Morse potential (eq 1). The Morse parameters for each bead type are listed in Table 3; we used geometric combination rules to compute the parameters of the cross interactions:

$$D_{o,ij} = \sqrt{D_{o,i}D_{o,j}}, \quad R_{o,ij} = \sqrt{R_{o,i}R_{o,j}} \quad \text{and} \quad \alpha_{ij} = \frac{1}{2}(\alpha_i + \alpha_j) \quad (2)$$

The nonbond interactions were truncated with a spline function, using a cut off radius of $R_{cutoff} = 12$ Å. The details of the force field development can be found elsewhere.[22]

With M3B, the MD simulations use time steps of 10 fs (10 times higher than for atomistic simulations of sugars), and the number of particles decreases by a factor of 8. In addition there is not need for the costly Ewald sums associated with coulomb interactions. The result is that MD simulations with M3B are about 7000 times faster than those for the fully flexible atomistic model.[22]

To study water structure in concentrated mixtures,we prepared concentrated glucose−water amorphous solutions with water content in the range 8−20 wt %, using the same composition and number of molecules as the atomistic cells (Table 1). Five independent coarse grain amorphous cells were prepared per water content. The M3B mixtures were constructed with the Cerius2 Amorphous Builder and equilibrated under isobaric−isothermal conditions at $p = 1$ atm and $T = 343$ K for 2 ns each. The first nanosecond was considered to be equilibration and the second nanosecond was used to extract the equilibrium properties. A bigger cell of composition 12.2 wt % water−glucose was prepared for determining the glass transition temperature and to study the dynamics over a broad range of temperatures. This larger periodic cell was composed of 90 glucose and 125 water molecules. The mixture was prepared and equilibrated at 343 K following the same procedure as for the other coarse grain cells.

For the system with 90 glucose + 125 water molecules, we performed NPT molecular dynamics simulations at temperatures $T = 365, 335, 310, 280,$ and 250 K. The equilibrated samples were run for times up to 0.65 μs.

3. Results and Discussion

3.1. Structure of Water in Glucose Mixtures. The M3B force field was developed[22] to reproduce structural (density, bond distances, etc.) and thermodynamics properties (energy vs V and V vs p) of amorphous glucose, and to reproduce the
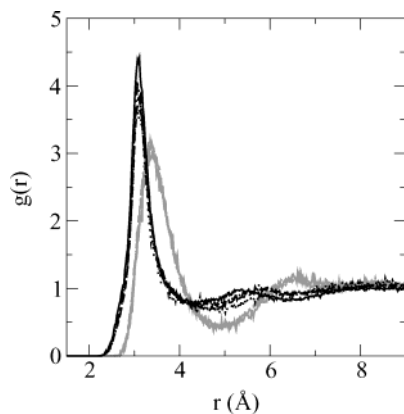
Figure 2. Water radial distribution function for the atomistic (black) and coarse grain (gray) water−glucose mixtures. For each model, $g(r)$ is rather insensitive to water concentration for the water contents considered. Thus, the lines for 8 (solid), 12.2 (points), 16.5 (dashed), and 20 wt % (dot−dashed) overlap for most of the r range.

density, cohesive energy and diffusion coefficient of pure water. Table 1 shows that M3B performs very well in predicting the densities of binary mixtures, giving values within 2−4% of the atomistic results.

In this subsection, we study the structure of water in concentrated water−glucose mixtures with two main purposes:

(1) First we evaluate the fidelity of the coarse grain model in predicting the structure of mixtures not considered in the force field parametrization. This comparison of atomistic and coarse grain models is done through the simultaneous analysis in the equilibrated mixtures of the (i) density, (ii) radial distribution function, (iii) water connectivity, and (iv) water percolation threshold for the same compositions.

(2) Second (and more interesting) is the characterization of the distribution of water in the highly hydrophilic environment provided by the sugars. In our atomistic simulation analysis of water−sucrose mixtures,[11] we found that water forms extended clusters that percolate into a 3D network for water contents above 18 wt % In this work, we present a similar analysis of water distribution in glucose, in the narrower range of 8−20 wt % water.

The radial distribution function (rdf) of water molecules is shown in Figure 2. The atomistic water−water distribution shows a first neighbor peak expanding up to ∼4 Å. This expansion of the first neighbor shell with respect to pure water has previously been observed for other low water content monosaccharides[13] and sucrose.[11,29] The radial distribution function for water in the coarse grain representation shows a good agreement, although the coarse grain model displays a broadening and displacement of the peak to larger distances. The lack of agreement between the details in the atomistic and coarse grain rdf is not surprising, since the parametrization of coarse grain water was done to reproduce the experimental properties of density, cohesive energy and diffusion of water at 300 K. It has been demonstrated[30] that two-body approximations of many body interactions (as in the case of a coarse graining procedure) cannot reproduce the rdf and the thermodynamics simultaneously. Although the details of the atomistic rdf are not reproduced by the coarse grain model, a close inspection of the distribution of water molecules in glucose mixtures reveals the similarity between the two models. For both the atomistic and coarse grain models, the water distribution is heterogeneous in a length-scale of a few molecular diameters. For both models we find similar water clustering in glucose, for example: two water molecules belong to the same cluster
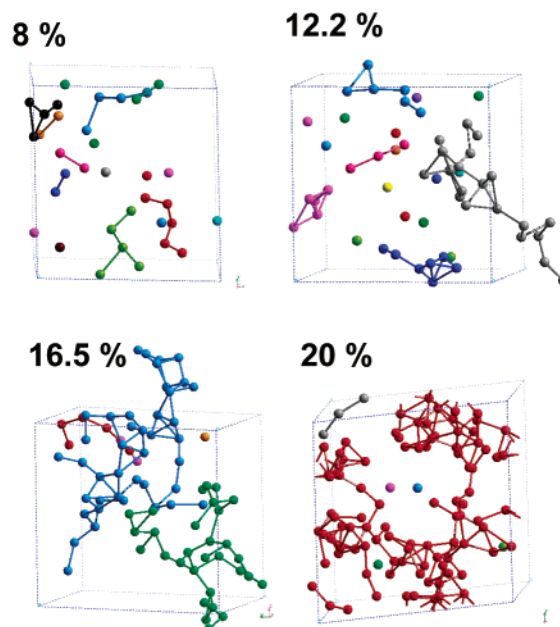

Figure 3. Typical configurations of water clusters in glucose solutions for various water content (wt % of water indicated on top of each snapshot). Each cluster can be identified by tracing the bonds between its constituents. The color of each cluster is arbitrary; it was assigned randomly. Water (balls) form scattered clusters (connected balls) with chainlike and starlike portions that grow with water content. The results shown here correspond to randomly selected snapshots for the atomistic models; water distribution for the M3B models does not look distinguishable at a glance from the atomistic ones.

if their oxygen atoms (or W beads, for the M3B model) are at a distance not farther than 4 Å. Although previous atomistic MD studies of water−glucose mixtures[13,31,32] analyze clusters in terms of standard hydrogen bonds distances and angles, our criteria for clusters is based only on distances because our goal is to characterize the connectivity of water irrespective of their possible orientations. The same spherical averaging is implicit in the use of a single particle model for water molecule in the coarse grain model.

Figure 3 displays the water molecules in atomistic water−glucose mixtures at different water contents. Lines connect water molecules that belong to the same cluster. A visual inspection of the clusters in the M3B model shows features indistinguishable from the atomistic description. To quantify the distribution of the molecules in the clusters, we define the connectivity for each water as the number of water neighbors within $d \leq 4$ Å. We computed the probability of a water molecule having n neighbors as an average over the four independent atomistic trajectories (five for coarse grain) for each water content. These distributions from the atomistic and coarse grain models (shown in Figure 4) are almost indistinguishable, suggesting that the distribution of the water molecules is determined more by the packing of the sugar component than by the details of the interaction potentials. We define a water cluster to be percolated if it is connected with its periodic image in the three axis directions. We computed the percolation probability as the fraction of percolated configurations over the set of four atomistic independent trajectories (or five coarse grain independent trajectories) of the amorphous mixture for each water concentration. The results (Figure 5) indicate that for *both* the atomistic and coarse grain model water percolation is attained between 16.5 and 20 wt % water. For atomistic water−sucrose mixtures, we found previously that the percolations threshold of water is between 10 and 18 wt % water for similar cell size
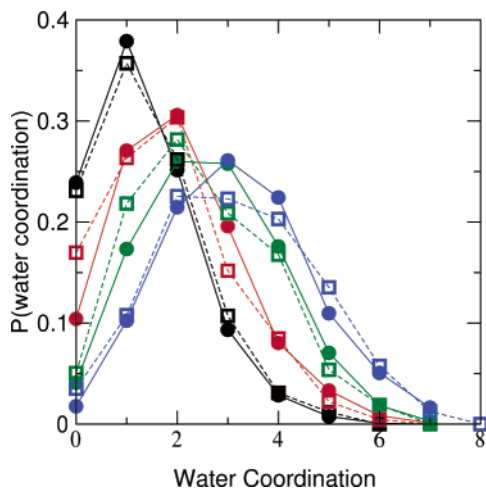
Mechanisms of Relaxation in Water−Glucose

J. Phys. Chem. A, Vol. 108, No. 17, 2004 **3703**

Figure 4. Water−water coordination distribution for water−glucose mixtures of various water contents. The atomistic (empty squares) and M3B (filled circles) distributions for 8% (black), 12.2% (red), 16.5% (green), and 20 wt % water (blue) show excellent agreement.
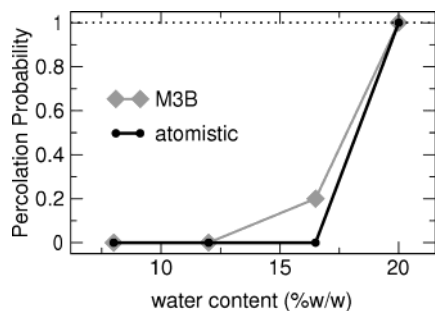

Figure 5. Percolation probability for water in glucose mixtures. The arrow provides a rough indication of the concentration at which percolation occurs. The clustering distance d was 4 Å. The simulation conditions are detailed in Table 1.

and temperature.[11] This suggests that the percolation threshold may be rather insensitive to the nature of the saccharide; in agreement with the hypothesis that for the concentration range studied here water distribution is mainly determined by the packing of the carbohydrates.

3.2. Translational dynamics for Water and Glucose. We will now examine in some detail the results for MD of glucose with 12.2 wt % water. We selected this water concentration for these studies, because it is a concentration for which water already form extended clusters while still presenting a considerable amount of isolated water molecules (WC = 0). This variety of water coordination environments is useful for testing whether water coordination has any impact on water mobility.

Concentrated glucose−water mixtures experience a transition between a viscous rubbery liquid and a glass at the glass transition temperature, T_g. This transition is accompanied by a change in thermal expansion coefficient. Hence, we estimated T_g from the intersection of the slopes of the glassy and rubbery regions of V vs $1/T$. The system was first equilibrated during 5 ns at 500 K at a constant pressure of 1 atm. It was then cooled to 200 K in steps of 50 K (0.5 ns at each temperature), equilibrated at 150 K for 10 ns and then heated in a series of steps in which the T was maintained during 125 ps, and then suddenly increased by 25 K, up to 325 K. Prior to the analysis of V vs $1/T$, the volume and temperature of the heating simulations were averaged every 5 ps to decrease the "noise" of the fluctuations. The resultant V vs $1/T$ curves are plotted in Figure 6, along with the linear fit for the two portions of low and high-temperature data. This method renders a $T_g^{M3B}{}_{12.2\%} =$
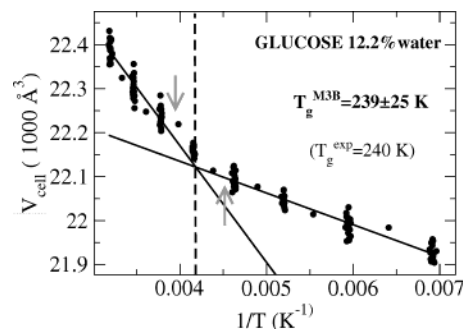

Figure 6. Determination of the glass transition temperature through the change in the thermal expansivity of the coarse grain 12.2 wt % water−glucose mixture. Ascending temperature stair of 25 K every 125 ps. The rubbery (high temperature) curve was fitted from the points left to the down pointing arrow, and the glassy (low T) curve from the points right to the up pointing arrow. See text for details.

239 ± 25 K for glucose with 12.2% w/w water with the M3B model. The predicted $T_g^{M3B}{}_{12.2\%}$ is indistinguishable from the experimental value, $T_g^{exp}{}_{12.2\%} = 240$ K,[33] within the error of our estimation. It should be noted, however, that the temperature rate used in the experiments (5 K/min) is many orders of magnitude slower than the one of the simulation. We studied the dynamics of glucose 12 wt % water at temperatures ranging from $T = 365$ to 250K, corresponding to T/T_g from 1.5 to 1.05. The simulation times spanned from 0.1 μs at 365 K to 0.65 μs at 250 K.

In the following we analyze the MD of water and glucose molecules with the aim of establishing the following points:

(i) The mechanism of water diffusion in glucose and how the mechanism changes when the system goes from a liquid to a deeply supercooled state.

(ii) The mechanism of glucose translational diffusion.

(iii) The relationship between water distribution and water dynamics in concentrated sugar solutions.

3.2.1. Mean Square Displacement. To quantify the extent of water and glucose mobility, it is useful to compute the time evolution of the mean square displacement (MSD) of the beads corresponding to the different species in the mixture. The MSD of a tagged particle is defined as $\langle r^2(t) \rangle = \langle |r(t) - r(0)|^2 \rangle$, where $\langle ... \rangle$ indicates an average over an equilibrium trajectory for the particles of a given species (i.e., glucose or water). Glucose MSD is defined in terms of the beads and not the center of mass mobility, so that it includes both translation and rotation of the glucose molecule. A log−log plot for the MSD for water and glucose is shown in Figure 7. They both show three distinctive regions:[34]

(i) For subpicosecond times a ballistic motion of the particles with $\langle r^2(t) \rangle \propto t^2$.

(ii) For intermediate times a plateau value of $\langle r^2(t) \rangle$, corresponding to the restricted motion of the particle within the cage formed by the sorrounding molecules.

(iii) At longer times a diffusional behavior $\langle r^2(t) \rangle \propto t^\nu$, where $\nu = 1$ for the hydrodynamic (Fickian) limit of long displacements or times. We observed that the hydrodynamic limit was not completely attained in the hundreds of nanoseconds of our simulations. Thus, for water, we found ν to range from 0.89 to 0.98 (see caption of Figure 8 for the ν values at each temperature).

The mobility of glucose beads is slower than those of water for each temperature, as expected from the size difference between these two molecules and in agreement with the experimental results.[9] The lower the temperature, the higher the separation of time scales of glucose and water diffusion. As an

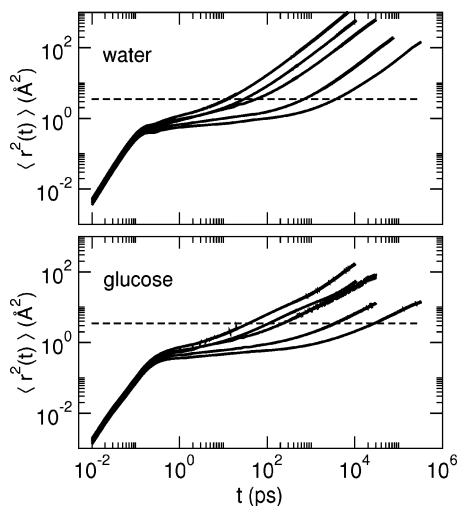**3704** *J. Phys. Chem. A, Vol. 108, No. 17, 2004*

Molinero et al.

Figure 7. Mean square displacement of water (upper panel) and glucose (lower panel) in 12 wt % water–glucose at T = 250, 280, 310, 335, and 365 K (from down up). The dashed line indicates 3.5 Å, approximately the size of a water molecule.
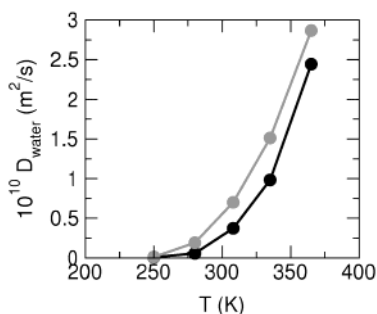

Figure 8. Water diffusion coefficient estimations, D_{app} (black circles) and D_{eff} (gray circles) for the 12 wt % water–glucose, computed with the M3B model. The values of the slope ν of the linear portions of water diffusion in Figure 7 were 0.98, 0.95, 0.93, 0.89, and 0.97 in decreasing order of temperatures.

example, we consider the time for which the MSD of water and glucose beads reach 3.5 Å (dashed lines in Figure 7):

(i) At T = 365 K, it takes 12.5 ps for water and 38 ps for the glucose beads.

(ii) At T = 250 K, it takes them 3.7 ns for water and 28.3 ns for the glucose beads.

For the range T = 310–365 K, the plateau region of MSD is not completely flat. But for T = 280–250 K, there is a very well-defined plateau of MSD for both for water and glucose. In analyzing water dynamics, we considered these two temperature ranges separately:

For T = 365–310 K, we classify the system as a moderately supercooled liquid,,

For T = 280 and 250 K, we classify the system as a deeply supercooled liquid.

More justification of this classification is given in section 3.2.2.

The water MSD attained in the plateau regions is comparable for all the temperatures: the amplitude of motion of each water molecule in the cage formed by its neighbors is ∼0.7–0.9 Å, increasing slightly with temperature. This amplitude for water vibration in the cage of neighbors is in good agreement with the 0.5–0.7 Å calculated for the H atoms of water molecules in disaccharides from QENS experiments.[35]

For times longer than the plateau region, we found $\langle r^2(t)\rangle \propto t^\nu$ for water diffusion. We estimated the diffusion coefficient for water in this third regime in two ways:
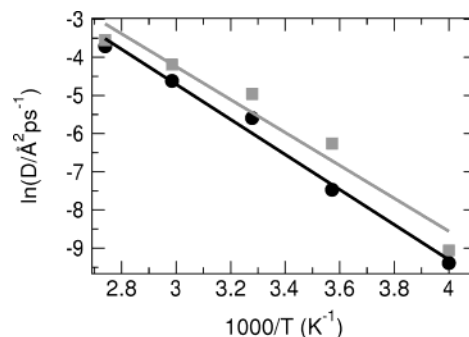

Figure 9. Arrhenius plot of the two estimations of the diffusion coefficient of water in 12% water–glucose. D_{app} (black circles) and D_{eff} (gray squares) of water in glucose 12 wt % water (see text for details). The lines correspond to the fits with the parameters indicated in Table 4.

TABLE 4: Arrhenius Parameters for Water Diffusion in a 12.2 wt % Supercooled Mixture

	D_{app}	D_{eff}
D_o(m²/s)	8.8×10^{-5}	5.9×10^{-5}
E_a (kJ/mol)	38.3 ± 2.3	35.8 ± 4.5

(i) An *effective* diffusional coefficient, D_{eff}, is defined by $\langle r^2(t)\rangle = 6D_{eff}t^\nu$, and

(ii) an *apparent* diffusion coefficients is computed by forcing ν to be 1, $\langle r^2(t)\rangle = 6D_{app}t$.

The values obtained are displayed in Figure 8. A similar analysis for glucose diffusion was not attempted in the present work because it would require much longer simulations to attain comparable quality of data. It should be emphasized that the D_{app} and D_{eff} are estimations of the diffusion coefficient, as ν should converge to 1 for long enough runs and the two estimations should converge to the actual diffusion coefficient. Thus, we may consider the difference between D_{app} and D_{eff} as indicative of the error bar in the estimated D.

To analyze the temperature dependence of water diffusion coefficient, we first considered an Arrhenius form:

$$D = D_o e^{-\frac{E_a}{RT}} \qquad (3)$$

Figure 9 displays an Arrhenius plot for the computed diffusion coefficients of water. Within the estimated uncertainty, the activation energy E_a and the preexponential D_o Arrhenius parameters obtained for D_{app} and D_{eff} (Table 4) are comparable:

$$E_a^{app} = 38.3 \pm 2.3 \text{ kJ/mol} \quad \text{and} \quad E_a^{eff} = 35.8 \pm 4.5 \text{ kJ/mol}$$

$$D_o^{app} = 8.8 \times 10^{-5} \text{ m}^2/\text{s}; \quad D_o^{eff} = 5.9 \times 10^{-5} \text{ m}^2/\text{s}$$

We were unable to find experimental diffusion coefficients for water in glucose with 12 wt % water content. The closest concentrations for which there are experimental determinations of water diffusion coefficient in the supercooled regime are 25 wt % glucose and 60 wt % water.[9] For these mixtures the Arrhenius equation provides a good fit for water diffusion, with

$$E_a^{25\%} = 31.1 \pm 1 \text{ kJ/mol} \quad \text{and} \quad E_a^{60\%} = 25.3 \pm 0.3 \text{ kJ/mol}^9$$

$$D_o^{25\%} = 1.7 \pm 0.8 \times 10^{-5} \text{ m}^2/\text{s} \quad \text{and}$$

$$D_o^{60\%} = 1.1 \pm 0.1 \times 10^{-5} \text{ m}^2/\text{s}$$

Considering the trend with decreasing water content, the preexponential factors and activation energy from our coarse

Mechanisms of Relaxation in Water−Glucose

J. Phys. Chem. A, Vol. 108, No. 17, 2004 **3705**

grain model is quite similar to the experiments, suggesting that the coarse grain description represents well the overall water mobility in supercooled glucose.

We also considered a Vogel−Fulcher−Tammann (VTF) temperature dependence of water diffusion coefficient,

$$D = Ae^{-\frac{B}{T - T_o}} \qquad (4)$$

This form is usually invoked for analyzing supercooled mixtures, and represents well the increasing temperature dependence of the dynamical quantities observed cooling to the glass transition. The temperature T_o is a phenomenological coefficient that is lower than T_g. We computed the values of A, B, and T_o coefficients from D_{app} and D_{eff} sets of data in the range 365−250 K. The results of unconstrained fits are

$$B = 2337 \text{ K} \quad \text{and} \quad T_o = 85 \text{ K} \quad \text{for } D_{app}$$

and

$$B = 501 \text{ K} \quad \text{and} \quad T_o = 190 \text{ K for } D_{eff}$$

It is evident that the parameters are too sensitive to the differences between D_{app} and D_{eff}. As these estimates of the diffusion coefficient should converge for sufficiently long trajectories, we interpret the calculated VTF parameters as bounds for the actual B and T_o parameters for water in this system. In this respect is encouraging to note that for water in 10 wt % water−sucrose the values extracted from experiment

$$B = 687 \text{ K} \quad \text{and} \quad T_o = 118 \text{ K}$$

lie between our two wildly different estimates. On the basis of this we fitted our results assuming $B = 687$ K to obtain $T_o = 176$ K for D_{app} and $T_o = 176$ K for D_{eff}. (correlation coefficients cc = 0.980 and 0.997, respectively). Alternatively assuming $T_o = 118$ K, our results lead to

$$B = 1557 \text{ K (cc} = 0.992) \quad \text{for } D_{app} \quad \text{and}$$

$$B = 1640 \text{ K (cc} = 0.997) \quad \text{for } D_{eff}$$

These results indicate that the accuracy of the simulations and the number of points are not sufficient to estimate the VTF parameters.

3.2.2. Van Hove Self-Correlation Function and Incoherent Intermediate Scattering Function. While the analysis of the MSD proves to be a very useful tool to examine the average displacement as a function of time, a more detailed analysis of molecular mobility is needed to establish the mechanism of water and glucose diffusion in supercooled mixtures. A suitable function to provide more insight into the motion of the particles is the van Hove self-correlation function, which indicates the probability density for a type of molecule to travel a distance r in a time interval t,

$$G_s^\alpha(r,t) = \frac{1}{N_\alpha}\langle\sum_{i=1}^{N_\alpha}\delta(r - |\vec{r}_i(t) - \vec{r}_i(0)|)\rangle \qquad (5)$$

where α = water (W) or glucose (G), $\delta(r)$ is the Dirac δ function, and $\langle...\rangle$ indicates a trajectory average. In the hydrodynamics limit[36] corresponding to $r \rightarrow \infty$ and $t \rightarrow \infty$ (Fickean

diffusion), the van Hove self-correlation function is a Gaussian function (eq 6)

$$G_s^\alpha(r,t) = \frac{1}{(4\pi Dt)^{3/2}}\exp\left(-\frac{r^2}{4Dt}\right) \qquad (6)$$

Incoherent neutron scattering experiments provide data on the incoherent intermediate scattering function $F_s(k,t)$, which is the space Fourier transform of the van Hove self-correlation function. Thus, we computed $F_s(k,t)$ as the isotropic Fourier transform of $G_s(r,t)$. In the hydrodynamic limit $F_s(k,t)$ is a single exponential,

$$F_s(k,t) = \exp(-Dk^2t) \qquad (7)$$

where D is the diffusion coefficient. A common, phenomenological, way to characterize the departure of $F_s(k,t)$ from the exponential regime, is its description as a KWW or stretched exponential (SE) function,

$$F_s(k,t) = e^{-(t/\tau)^\beta} \qquad (8)$$

The exponent β is called the nonexponential parameter, with values between 0 and 1, while fitting parameter τ is associated with an effective time constant $\bar{\tau}$ through

$$\bar{\tau} = \frac{\tau}{\beta}\Gamma\left(\frac{1}{\beta}\right) \qquad (9)$$

where Γ is the gamma function. The description of $F_s(k,t)$ by a stretched exponential function is not valid in the ballistic regime, since $F_s(k,t)$ has a quadratic dependence on time.[37] Thus, we discard the first picosecond of $F_s(k,t)$ decay in our analysis, effectively assuming that $F_s(k,t) = A(k)e^{-(t/\tau)^\beta}$. We will not analyze the behavior of $A(k)$ here, but rather focus on the nonexponential parameter β and the characteristic time $\bar{\tau}$.

The MSD of glucose shown in Figure 7 corresponds to the average of translational motion of the three beads in the M3B representation of the glucose molecule and has contributions both from the center of mass (CM) translation and the rotation of the molecules. To determined the CM contribution to glucose mobility, we used the van Hove self-correlation function, $G_s^G(r,t)$, defined by eq 5, where r indicates the position of glucose molecule center of mass.

In the following we will examine the diffusion of water and glucose in this concentrated mixture as a function of temperature from the moderate to the deep supercooled state.

3.2.2.1. Translational Dynamics in the Moderately Supercooled Regime, $T = 310-365$ K. Figure 10 shows $G_s^W(r,t)$ for water in 12 wt % water−glucose at 365, 335, and 310 K at a variety of times spanning over the semi-plateau region of Figure 7 into the diffusive regime. At long times the curves tend to a Gaussian $G_s^W(r,t)$, but for short times an evident shoulder is seen at distances around 3.5−4 Å, along with a persistent first peak. The departure of the van Hove self-correlation function from Gaussian can be quantified through the non-Gaussian parameter α_2,[38] defined in terms of the lowest moments of $G_s(r,t)$

$$\alpha_2(t) = \frac{3\langle r^4(t)\rangle}{5\langle r^2(t)\rangle^2} - 1 \qquad (10)$$

For a Gaussian distribution $\alpha_2(t)$ is zero.

Figure 11 compares the non-Gaussian parameter $\alpha_2(t)$ for water and glucose in the 12 wt % water mixture at the highest
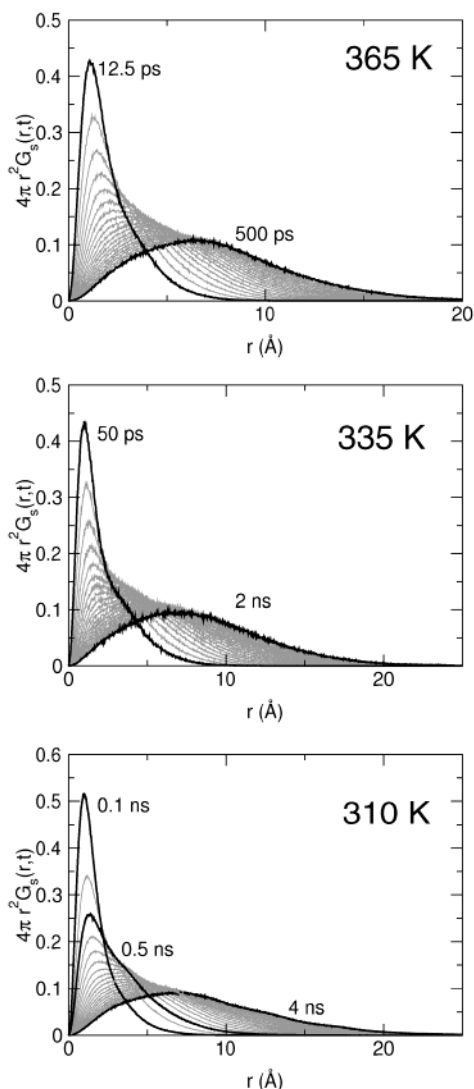
3706 *J. Phys. Chem. A, Vol. 108, No. 17, 2004*

Molinero et al.

Figure 10. Van Hove self-correlation function for water in 12.2 wt % water−glucose for the moderately supercooled regime (310−365 K). Note at distances of ∼3.5−4 Å the presence of a shoulder on the main (diffusive) peak. The position of the shoulder is comparable to water size (see Figure 2) suggesting the existence of preferential jump distances for the water molecules.
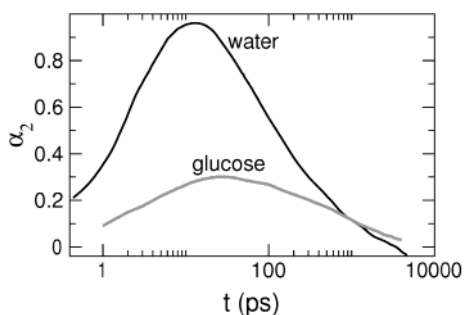

Figure 11. Non-Gaussian parameter α_2 (eq 10) for translational diffusion of water and glucose at $T = 365$ K in 12 wt % water−glucose. This shows higher non-Gaussianity for water than glucose.

temperature, 365 K. We see here that water dynamics departs more from the hydrodynamic behavior than glucose, although glucose diffusivity is slower. For water at 365 K, the maximum departure from Gaussian behavior is at $t^* = 13$ ps. Figure 12 compares the actual van Hove function for water at $t = 10$ ps in the glucose mixture at 365 K with the Gaussian prediction for the hydrodynamic value of the diffusion coefficient (D_{app}
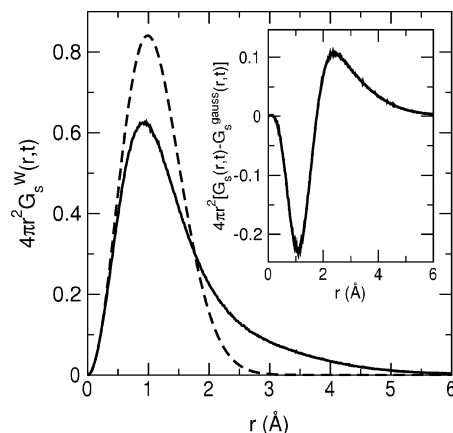

Figure 12. Van Hove self-correlation function for water $4\pi r^2 G_s(r,t)$- for $t = 10$ ps at $T = 365$ K (solid line) compared to the Gaussian prediction $4\pi r^2 G_s^{gauss}(r,t)$ for the same t (dashed line) from eq 6 [using the diffusion coefficient $D = 0.024$ Å^2/ps obtained from the long time slope of MSD (Figures 7 and 8)]. The difference between the two curves (inset) reflects the contributions from jumps, leading to a distribution of distances between ∼2.5 and 4 Å for the decay of water $4\pi r^2 G_s(r,t)$.
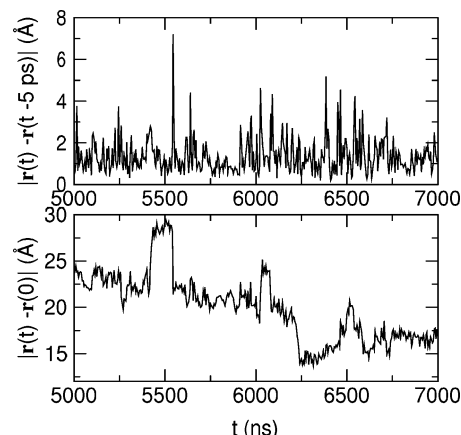

Figure 13. Occasional jumps for a randomly selected water molecule at 365 K (upper panel) and the effect of these jumps on the cumulative displacement of that molecule (lower panel). Water motion consists of continuous small steps, associated with continuous diffusion, combined with jumps.

$= 0.024$ Å^2/ps at $T = 365$ K). The difference between the two curves (inset of Figure 12) suggests that there is a second water diffusion mechanism in addition to regular diffusion. To analyze the incidence of jumps in the mechanism of water diffusion at 365 K, we followed the individual molecule displacements using a time resolution of 5 ps. The displacements for a randomly selected water molecule are shown in Figure 13. This shows that water experiences both small and big jumps, consistent with a jump diffusion mechanism.

The non-Gaussian van Hove self-correlation functions shown in Figure 10 correspond to nonexponential incoherent intermediate scattering functions $F_s^\alpha(k,t)$. We analyzed $F_s^\alpha(k,t)$, the CM translation for water and glucose using 19 equispaced k values in the range 0.25−2.5 Å^{-1}. This range covers the reciprocal distances $r = 2\pi/k$ from 2.5 to 25 Å. The stretched exponential function (eq 8) gives an excellent fit for the time decay of $F_s^\alpha(k,t)$ at $T = 310$−365 K for all reciprocal distances studied. We observe in Figure 14 that the stretch exponent β for water translation is lower than 1 in throughout the k range studied. We also find that for each temperature, the water relaxation is more nonexponential than is glucose relaxation; i.e., β for water is lower than β for glucose. The wave vector dependence of β

Mechanisms of Relaxation in Water−Glucose

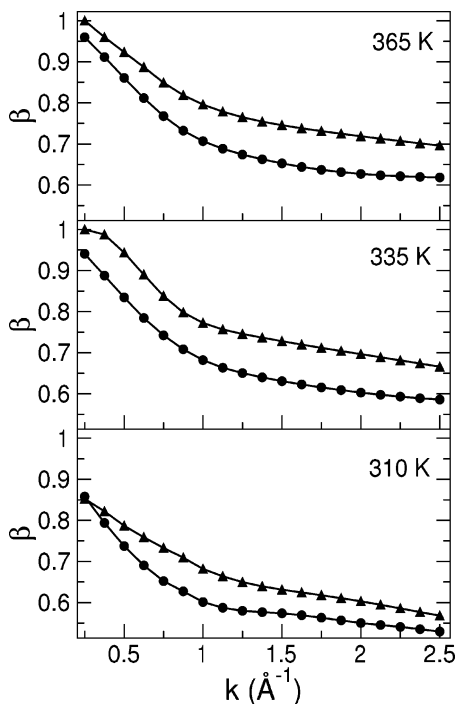*J. Phys. Chem. A, Vol. 108, No. 17, 2004* **3707**

Figure 14. Stretch exponent β for the nonexponential relaxation of water (circles) and glucose (triangles) in the moderately supercooled regime (310−365K) for the water−glucose mixture. β is lowest for the molecular size distances ($k \geq 1$ Å^{-1}), where the heterogeneous structure of the mixture is more pronounced. Beyond the molecular size, there is a steep increase of the nonexponential parameter toward 1.

is similar for both components and for all the three temperatures. We found that β vs k displays a "two-slope regime": β presents a low, slowly varying value up to $k \sim 1$ Å^{-1} and then increases steeply in the range of distances above the molecular size. Considering β as a measure of the dynamical heterogeneities in the mixture (see below), Figure 14 reveals that an important contribution to the heterogeneity of the dynamics of glucose and water is to be found in the heterogeneous first neighbor structure of the mixture (Figure 3).

Stretch exponents lower than one can arise from a distribution of exponential decays (called the heterogeneous scenario) or from subdiffusive behavior of all the particles (homogeneous scenario). In the heterogeneous scenario there is a distribution of time constants for the mobility. In this context, a lower β implies a broader distribution of characteristic times. Arbe et al.[39] proposed to distinguish between a homogeneous and heterogeneous scenario by the power exponent n of the wave vector dependence of the inverse average time scale, $\bar{\tau}^{-1} \propto k^n$:

(i) If the distribution is a sum of exponential decays, then $n = 2$.

(ii) If the diffusion is homogeneous and subdiffusive, $n = 2/\beta$.

3.2.2.1a. Translational mobility of Glucose CM. Figure 15 shows that $n = 2$ for the glucose CM translation at 365, 335, and 310 K throughout the k range studied. This indicates that the glucose nonexponential intermediate scattering function can be understood as a superposition of exponential (continuous diffusive) relaxations with a broad range of time scales. The average translational diffusion coefficients for glucose can be estimated from

$$\bar{\tau}^{-1} \propto Dk^2 \qquad (11)$$

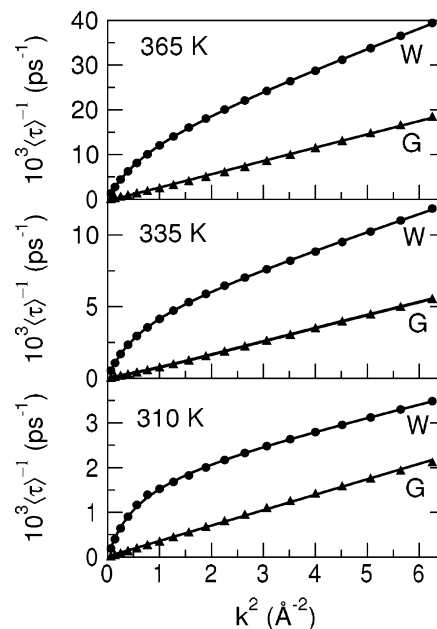The computed characteristic times for glucose translation

Figure 15. Wavevector dependence of the characteristic translational time. Circles and triangles correspond to the simulation results for water and glucose translation, respectively. The lines correspond to the fit to a model of random jump model plus continuous diffusion for water (eq 13) and a continuous diffusion for glucose center of mass (eq 11).

TABLE 5: Translational Diffusion Characteristics for Water and Glucose[a]

T (K)	water				glucose D (Å^2/ps)
	$\bar{\tau}_o$ (ps)	l_o (Å)	D^{jump} (Å^2/ps)	D^c (Å^2/ps)	
365	72.6	2.77	1.8×10^{-2}	4.3×10^{-3}	2.9×10^{-3}
335	211.6	3.16	7.9×10^{-3}	1.2×10^{-3}	8.7×10^{-4}
310	514.6	3.28	3.5×10^{-3}	2.7×10^{-4}	3.5×10^{-4}
E_a (kJ/mol)	32.0 ± 2.3		26.8 ± 0.6	45.4 ± 1.2	34.6 ± 3.4

[a] $D^{jump} = l_o^2/6\bar{\tau}_o$ is the low k-vector contribution to the diffusion coefficient due to water jumps, shown for comparison with the continuous component D^c. The activation energy E_a shown in the last row corresponds to an Arrhenius analysis of the respective time constants and diffusion coefficients.

provide an excellent fit to eq 11 (straight lines through triangles in Figure 15). The estimated diffusion coefficients for glucose are listed in Table 5.

We computed the apparent activation energies for CM diffusion in glucose from the diffusion coefficients at three points in the range 310−365 K. The activation energy obtained from this method, $E_a = 34.6$ kJ/mol) (see Table 5) is comparable to that ($\sim$35 kJ/mol) obtained for water diffusion. This result disagrees with the experimental available information for glucose diffusion,[9] which shows that the activation energy for glucose diffusion increases with the sugar concentration and is already 54 kJ/mol for the 25 wt % water glucose mixture. We interpret this as indicating that the low activation energy we compute for glucose is an artifact of our coarse grain model, which accounts for the effect of the hydrogen bonds using a mean field. For a concentrated glucose solution, we expect that sugar will form a hydrogen bond network,[22] and that the topological constraints of the multiple sugar-sugar hydrogen bonds will decrease glucose mobility, thus increasing the activation energy above that of water.

3.2.2.1b. Translational Mobility of Water. Water $\bar{\tau}^{-1}$ values (circles in Figure 15) show an initial linear behavior of $\bar{\tau}^{-1}$ vs k^2, followed by a flattening for higher k that cannot be

represented as $\bar{\tau}^{-1} \propto k^{2/\beta}$ (all attempts to obtain a linear fit lead to an unphysical $\beta > 1$). This flattening of $\bar{\tau}^{-1}$ is indicative of a jump-diffusion mechanism and has been observed for water diffusion in neutron scattering experiments of trehalose[7] and fructose[8] solutions. A random jump-diffusion model[40] in which the particles wait for a time $\bar{\tau}_o$ between jumps of length l_o predicts that

$$\bar{\tau} = \bar{\tau}_o\left(1 + \frac{6}{k^2 l_o^2}\right) \tag{12}$$

According to this equation, $\bar{\tau}$ reaches a constant value at high k values corresponding to the time between jumps, $\bar{\tau}_o$. Our simulations indicate that $\bar{\tau}$ for the water beads increases even beyond $k = 2.5$ Å^{-1}, in agreement with neutron scattering data for water in carbohydrates.[7,8,35,41] If we assume that water can translate either via jumps or via continuous diffusion, the rate constant of translation can be writen as a sum of a rate constant due to jumps (eq 12) plus a rate constant due to small-step continuous diffusion:

$$\frac{1}{\bar{\tau}} = \frac{1}{\bar{\tau}_o}\left(\frac{k^2 l_o^2}{6 + k^2 l_o^2}\right) + D^c k^2 \tag{13}$$

Equation 13 gives an excellent fit for $\bar{\tau}^{-1}$ of water, as shown in Figure 15 (the circles indicate data points, the lines through them are the fits). Table 5 lists the parameters corresponding to the following:

(i) The waiting time between jumps $\bar{\tau}_o$.

(ii) The length of the jumps l_o.

(iii) The effective contribution to the diffusion from small-step (continuous) diffusion, D^c.

We observe that the length of the jumps decreases with increasing temperature and is comparable to the size of the water bead at the lower temperatures. The jump-diffusion model analysis of neutron scattering experiments in supercooled water found the same trend of increasing jump length with increased supercooling.[42] We estimated the temperature dependence of diffusion in terms of an Arrhenius function for continuous diffusion, D^c, and the form $D^{jump} = l_o^2/6\bar{\tau}_o$ for jump contributions. The ratio D^{jump}/D^c was 13, for $T = 310$ K, 6.6 for 335 K, and 4.2 for 365 K. This trend (see the computed activation energies in Table 5) shows an increasing relative contribution of the jump mechanism to water diffusion as the temperature decreases, but a longer waiting time between hops.

3.2.2.2. Translational Mobility in the Deep Supercooled Mixture: $T = 250-280$ K. The preeminence of the hopping mechanism for water diffusion in glucose at the lowest temperatures produces distinctive secondary peaks in the van Hove self-correlation function. At $T = 310$ K, $4\pi r^2 G_s^W(r,t)$ showed a significant shoulder on a single peak whose maximum evolves with time to larger distances, but at $T = 280$ K the shape of $4\pi r^2 G_s^W(r,t)$ displays an almost stationary first peak with a well-defined secondary peaks that grows at the expense of the first one (upper panel of Figure 16). The first peak corresponds to the vibration of the water molecule in the "cage" formed by its neighbors, and its position is invariant at the lowest temperature. The position of this first peak in $4\pi r^2 G_s^W(r,t)$ corresponds to the distance observed in the plateau of $\langle r^2(t)\rangle$ (see Figure 7). The position of the second maximum of $4\pi r^2 G_s^W(r,t)$ at $r \sim 3.7$ Å is comparable to the closest water–water and water–glucose distances.

We computed the intermediate scattering functions $F_s(k,t)$ for water at 280 K, and found that its time evolution can be
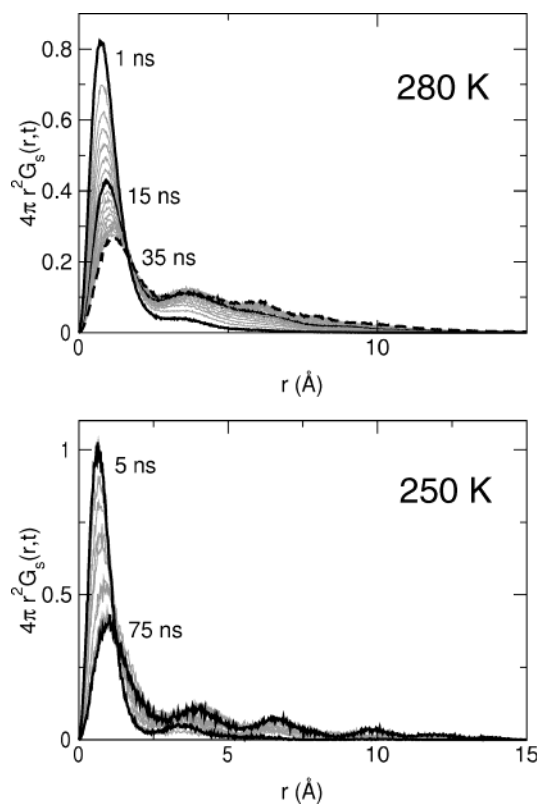

Figure 16. Van Hove self-correlation function for water in 12 wt % water–glucose at $T/T_g = 1.17$ and 1.05 showing well-defined peaks that indicate a jump mechanism for water mobility. The existence of multiple jump peaks is a consequence of the separation of water and glucose translational time scales in the 12 wt % water–glucose mixture.

TABLE 6: Characteristic Time Scales $\bar{\tau}$ and Stretch Exponents β for Water Translation, for $k = 1.75$ Å^{-1}

T (K)	$\bar{\tau}$ (ps)	β
280	10 078	0.52
310	403	0.56
335	131	0.62
365	41	0.64

represented by the stretched exponential function (eq 8). Table 6 lists the characteristic times $\bar{\tau}$ and stretched exponents β for water translation at $k = 1.75$ Å^{-1}, the reciprocal distance of the first hopping peak, in the range 280–365 K. The characteristic time at 280 K is ~10 ns.

Notwithstanding the good agreement of the diffusion coefficient temperature dependence with the Arrhenius equation for all the temperatures studied, the characteristic jump times at $k = 1.75$ Å^{-1} do not follow an Arrhenius form in the range 365–280 K: While an E_a of 37.33 kJ/mol can be computed from the three highest temperature $\bar{\tau}$, the apparent E_a for water translation between 310 and 280 K is more than double this value (82.4 kJ/mol).

The van Hove self-correlation function for water at the lowest studied temperature, $T = 250$ K (Figure 16), shows the same qualitative features as for $T = 280$ K, but with more pronounced: multiple peaks whose positions do not evolve on the hundred nanoseconds time scale. The existence of well-defined peaks in $4\pi r^2 G_s^W(r,t)$ is indicative of a hopping mechanism for water mobility in the deeply supercooled glucose mixture. We tested the existence of this mechanism by calculating the displacements of individual water molecules. The distances $d_i(t) = |\vec{r}_i(t) - \vec{r}_i(0)|$ traveled at 250 K for several randomly chosen water molecules are shown in Figure 17. This figure confirms

Mechanisms of Relaxation in Water−Glucose

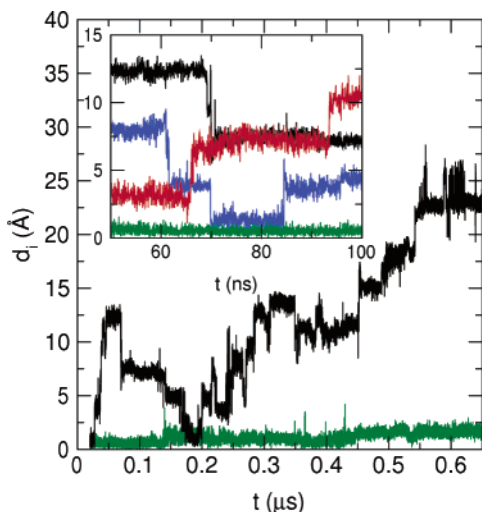*J. Phys. Chem. A, Vol. 108, No. 17, 2004* **3709**

Figure 17. Displacement $d_i(t) = |\vec{r}_i(t) - \vec{r}_i(0)|$ of the least moving (green) and most hopping (black) water molecule during the 650 ns simulation. The inset displays the displacement of these two molecules plus two other randomly selected molecules, in a shorter time frame.
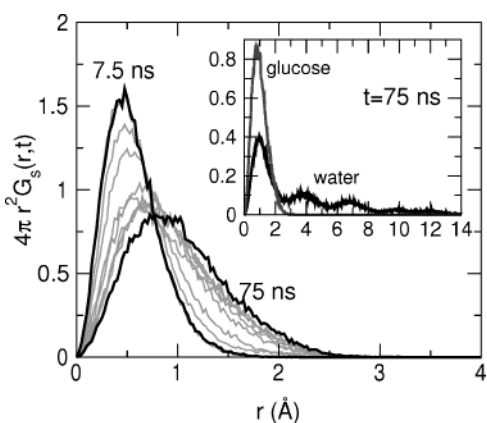

Figure 18. Van Hove self-correlation function $4\pi r^2 G_s^G(r,t)$ for glucose center of mass mobility at 250 K. The translation of glucose center of mass does not show secondary peaks even at the lowest temperatures. The inset shows the differences in displacement of water and glucose after 75 ns.

that, at 250 K, water in 12 wt % water−glucose moves through simple hops of about 3.5 Å. The small step diffusive mechanism that is significant in the moderately supercooled liquid regime (see Figure 13 and Table 5) does not contribute to water translation close to the glass transition. On cooling the jump-diffusion mechanism for water gives rise to a hopping mechanism. Another feature obvious from Figure 17 is that there is a wide distribution of waiting times between water jumps. After 0.65 μs some water molecules still have not moved from their initial position, while others jumped hundreds of times.

In contrast the translation of the glucose center of mass at 250 K does not show evidence of jumps comparable to the beads sizes. Glucose $4\pi r^2 G_s^W(r,t)$ displays only one peak (Figure 18) whose r_{max} position advances slowly with time, corresponding to a diffusive motion. The behavior we observe for glucose dynamics in this mixture is similar to the behavior for *o*-terphenyl (OTP) in the model of Lewis and Wahnstrom.[43] The similarity is not surprising since our model for glucose molecule and their model for OTP consist of three beads in a similar geometry. The overall translational mobility of glucose at 250 K is negligible compared with water (see inset of Figure 18), supporting the idea that at the lowest temperatures there is an increasing separation of the time scales of water
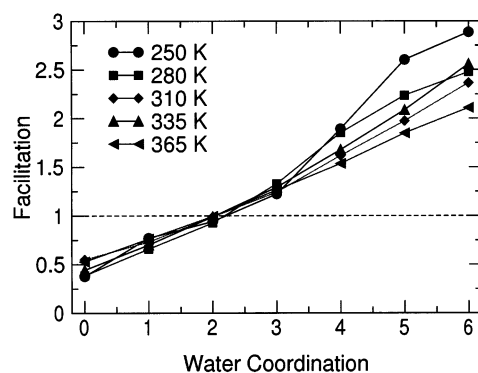

Figure 19. Water coordination facilitates water mobility. *Facilitation* is defined by eq 14.

and glucose diffusion, leading to migration of water between discrete positions in a matrix that is translationally frozen in that time scale. Even after traveling for distances on the order of four molecular diameters, the water molecules at 250 K still show preferential positions evidenced as local maxima in the $4\pi r^2 G_s^W(r,t)$.

3.3. Water Facilitation: The Effect of the Heterogeneous Structure on the Dynamics. We showed in section 3.1 that water distribution in concentrated glucose is heterogeneous at the molecular length scale (Figures 3 and 4), and in section 3.2 that water dynamics is nonexponential, especially at molecular size reciprocal distances (Figure 14). Now we discuss the relationship between these structural and dynamical heterogeneities. The locally heterogeneous structure of water in glucose implies the existence of a distribution of local environments. Here we characterize the water environment by a single variable: the number of other water molecules closer than 4 Å (defined as water coordination). The increasing separation of characteristic times between water and glucose translation at the lowest temperatures suggests that this variable for water dynamics in the supercooled and glassy state may be sensitive to the connectivity between water molecules.

To analyze the effect of water coordination in water dynamics we computed the following:

(i) The distribution $P(WC)$ of all the water molecules for each of the equilibrium trajectories of 12.2 wt % water mixtures at $T = 250$ to 365 K (analogous to the results shown in Figure 4).

(ii) The distribution describing the coordination of the water molecules *when they jump*, $J(WC)$, where we considered that a jump occurs when a molecule moves at least 3 Å in 20 ps.

$J(WC)$ considers only the coordination of the water molecules just before they jump. If the jumps were independent of water coordination, the ratio between $J(WC)$ and $P(WC)$ should be 1 for all WC. We define the ratio between these two distributions as the *facilitation*

$$facilitation(WC) = \frac{J(WC)}{P(WC)} \qquad (14)$$

The *facilitation* for water mobility in 12.2 wt % water−glucose is shown in Figure 19 for the five supercooled temperatures. The results show the dramatic effect of water coordination on water dynamics: The probability that a water molecule jumps increases almost linearly with their number of water neighbors. The probability for an isolated water in the sugar matrix (WC = 0) to move one water diameter in 20 ps is less than half the value it would have if the process were independent of water coordination. In contrast, the jump probability of water is double the average if its coordination is

above 5. These results indicate that the free energy barriers for the activated water diffusion are decreased by the presence of water neighbors. The effect of temperature in the facilitation is reasonable: the higher the temperature, the more mobile the glucose matrix and the less relevant is the water−water coordination for the water mobility. However these results show that even at $T = 365$ K, the mixture is still in a landscape influenced dynamical regime and that the structure-induced barriers still play an important role. This result is in agreement with the existence of true jumps in the dynamics of water even at such relatively high temperatures.

The presence of dynamical heterogeneities in water mobility is expected to produce a nonexponential relaxation of the intermediate scattering function and a broad distribution of waiting times between jumps. These two effects have been observed for water diffusion in the 12.2 wt % water−glucose solution, and we consider them to be manifestations of the microscopic heterogeneity of water structure in these mixtures. This picture agrees with the temperature dependence of the nonexponential parameter β: At lower temperatures, the mobility depends more on water coordination, leading to a broader distribution of time scales that produces a lower β for water. It is tempting to attempt an equivalent analysis for the k dependence of β (Figure 14). In this case it seems that the main contribution to the heterogeneous dynamics arises from short distance molecular interactions ($k > 1$ Å^{-1}), in agreement with the change of the mobility with water coordination in the first shell. A more thorough analysis is required, however, to assess the effects of longer range water structure in the heterogeneous dynamical response and the microscopic interplay between water and glucose dynamics in these mixtures.

4. Summary

In this work, we present atomistic and coarse grain simulations of the distribution of water in concentrated glucose mixtures and a coarse grain study of the translational dynamics of water and glucose in the supercooled regime. We find a relationship between the heterogeneous structure of water in these mixtures and its heterogeneous dynamics. The main findings are ars follows.

4.1. Structure. The M3B coarse grain model, parametrized to fit the atomistic properties for pure glucose and water, [22] gives densities for concentrated water−glucose mixtures at $T \sim 340$ K that are within 2−4% of the results from the atomistic model (Table 1). The atomistic distribution of water in glucose mixtures is also well reproduced by the coarse grain model, leading to a heterogeneous water structure at the length scale of a few water diameters. Similar results were found previously for atomistic simulations of aqueous solutions of fructose[13] and sucrose.[11] The water structure consists of clusters with chain and starlike portions that we characterize through the distribution of water−water connectivity, P(WC). The distributions obtain from the atomistic and coarse grain models (Figure 4) agree surprisingly well for all water contents (8−20 wt %) studied. Moreover, the two models predict the same percolation threshold for water in glucose, between 16.5 and 20 wt % at $T = 340$ K (Figure 5). This agreement between the coarse grain and atomistic results shows that the main features in the water distribution in concentrated glucose is described well *without* include explicitly directional water−water interactions (such as hydrogen bonds or a distribution of point charges). This suggests that the water structure in the mixture is *not* determined by directional water−water hydrogen bonds but rather is determined by the packing of water in the glucose matrix. Thus, the success

of our coarse grain model is due to its ability to reproduces very well the shape and interaction energy of glucose.[22]

The structures formed by water in glucose are similar to those observed in other carbohydrate mixtures.[11] Interestingly, they resemble the transient structures of highly mobile water molecules observed by Giovambattista et al. in atomistic simulations of pure supercooled water.[44] The similarity of these structures may be responsible for the T_o of the VTF analysis (eq 4) of the relaxation of water in concentrated sugar mixtures[45] being the same as the T_o for pure supercooled water. We consider that the origin of this coincidence may be the existence of similar mobile water cluster structures in a frozen medium. While the water clusters are dynamical and transient in the case of pure supercooled water where they move in a frozen water environment, the water clusters formed in the concentrated sugar mixtures are structural and relax in a frozen sugar structure. The similarity of the frozen sugar and water environment from the point of view of the relaxing water molecules may be responsible for confering similar dynamical characteristics to the two processes.

4.2. Dynamics. We have studied the dynamics of water and glucose in the mixture with 12 wt % water using the M3B coarse grain model. The glass transition temperature of the mixture computed with the coarse grain model (239 K) is indistinguishable from the experimental value (240 K) (Figure 6). We studied the translational dynamics in the T/T_g range 1.5−1.05. Throughout this temperature range, the log−log analysis the mean square displacement of water and glucose both show the characteristic plateau of supercooled liquids (Figure 7). For water, we obtained the diffusion coefficients from the long time behavior of the MSD and found that the temperature dependence is well described with an Arrhenius form (Figure 9). The computed activation energy for water diffusion is 35−38 kJ/mol. This result compares well with the expected activation energy from extrapolating the values for water diffusion in 25 and 60 wt % water−glucose mixtures obtained with NMR in the supercooled regime,[9] 31.1 and 25.3 kJ/mol, respectively. The preexponential factor also is in the same order of the experimental one,[9] indicating that the essentials of water mobility are well captured by our simple coarse grain model. We observed that for all temperatures the diffusion of water in 12.2 wt % water glucose is faster than that of glucose and that at room temperature it is about 2 orders of magnitude below the diffusivity of pure water. We find water diffusion to be nonexponential (Figure 14), in agreement with experimental dielectric relaxation results for water−glucose mixtures in the same concentration range[46] and with neutron scattering data for water in fructose.[8]

We find that the mechanisms for translational diffusion of water and glucose are different. The dynamics of glucose center of mass is nonexponential with no evidence of jumps for reciprocal distances up to 2.5 Å^{-1}. For glucose, the inverse of the characteristic time of translation versus k^{-2} is linear. This wave vector dependence of the characteristic time, (Figure 15) along with a $\beta^G < 1$ (Figure 14) is consistent with a dynamically heterogeneous scenario[39] in which the glucose molecules diffuse in a continuous way with a distribution of characteristic times. We find an activation energy for glucose diffusion in the range 365−310 K that is comparable to that of water (Table 5). The trend of experimental activation energies of water and glucose in 25 and 60 wt % water mixtures[9] indicate that the glucose E_a should be considerably larger than that of water. While the coarse grain model reproduces very well the energetics of glucose−glucose interactions, it does not provide the "sticky points" that restrain glucose−glucose relative mobility. We

speculate that the absence of such directional interactions will prevent the system from forming a polymer-like structure[11] and may be the responsible for the discrepancy in the activation energy.

For water diffusion we considered two regimes:

(i) A moderately supercooled regime for $T/T_g = 1.3−1.5$.

(ii) A deeply supercooled regime below $1.2 \, T_g$.

These two regimes differ in the relevant contributions to water diffusion of a continuous diffusion component vs the importance of jumps (compare the time evolution of the peaks in the van Hove self-correlation functions in Figures 10 and 16).

In the moderately supercooled regime, water has two relaxation mechanisms:

(i) Continuous small step diffusion.

(ii) Big jumps of ∼3 Å average length that become longer and less frequent as the temperature is decreased.

Thus, we interpret the diffusion rate of water as a sum of a diffusion rate through random jump diffusion plus a diffusion rate through continuous diffusion (Figure 15). Jumps play a significant role in water diffusion in 12.2 wt % water−glucose even at $1.5T_g$. Notwithstanding the increase in the waiting time between jumps, we find that for water the jump mechanism increases in importance with decreasing temperature (Table 5). In the deep supercooled regime the predominant mechanism of water diffusion is through hopping. At 250 K, the characteristic times for glucose diffusion is much lower than that of water, and water hops in a translationally frozen matrix (see inset of Figure 18).

The appearance of well-defined peaks in the van Hove self-correlation function for T/T_g below 1.2, along with characteristic times on the order of a few nanoseconds, signals the onset of landscape controlled dynamics[47] in this system. In addition water−sucrose experiments show a breakdown of Stokes−Einstein relation[10] that suggests similar phenomena. Indeed a similar change in dynamics around $1.2T_g$ is also observed in molecular dynamics simulations of simple Lennard-Jones fluids.[47,48] Sastry et al.[47] showed that binary Lennard-Jones mixtures lead to an onset of nonexponential relaxation at a temperature below from which the depth of the potential energy minima explored by the liquid increases with decreasing temperature. They find a temperature below which nonexponential relaxation occurs so that above T_g there is an abrupt increase in the energy barriers separating energy minima leading to dynamics that is dominated by rare jumps on the order of the interparticle distance. This description is consistent with our findings for water translational dynamics in this binary mixture: the onset of nonexponential relaxation is above 365 K, and the loss of the continuous diffusion mechanism can be interpreted as the disappearance of the shallow energy minima. We identify the deep supercooled regime with the region of hopping preeminence.

We measured the nonexponential nature of the relaxation of water and glucose through the wave-vector dependent stretch-exponent β. We find (Figure 14) that (i) water relaxation is more nonexponential than that of glucose for all conditions, in qualitative agreement with NMR results for supercooled water−glucose mixtures,[9] (ii) the β for both water and glucose increase with temperature, and (iii) the wave-vector dependence of the stretch exponents is similar for the two components: β decreases sharply with increasing k, up to $k \sim 1$ Å^{-1} and then decreases slowly up to $k = 2.5$ Å^{-1}, the maximum wave vector studied. The latter range corresponds to the molecular size of water and glucose, indicating that the heterogeneities in the translational dynamics are felt particularly in the molecular range. This result

points to a possible relationship between the heterogeneous structure of water in glucose and the heterogeneous distribution of time scales expressed through low values of β.

We analyzed the relationship between the local structure of water and water mobility and found that the heterogeneous structure of water [characterized by the presence of a distribution of water−water coordination populations P(WC)] has a tremendous impact on water mobility. We showed that water−water connectivity facilitates water diffusion (Figure 19) and that the effect is more pronounced for the lower temperatures, where the dynamics of the glucose molecules is slowed with respect to water. The smoothing in the dispersion of the structural facilitation with increasing temperature is in agreement with the observed increase of the nonexponential parameter β for water with increasing temperature (Figure 14 and Table 6). We consider that the facilitation mechanism plays a very important role in the nonexponential nature of water relaxation. The fact that β is lower for reciprocal distances comparable to the molecular size strongly supports the relevance of this close-neighbors mechanism in the facilitation of mobility in supercooled mixtures.

A relationship between water local structure and water dynamics was previously found by Sciortino et al.[49,50] These authors studied atomistic liquid and supercooled water through molecular dynamics simulations and found that water molecules with five or six neighbors have higher mean square displacements than those with four neighbors. Although these papers unfortunately do not indicate whether the mobility for water with two or three neighbors is lower than for a perfect tetrahedral environment, the increase of mobility below a density ρ_{Dmin} (∼0.9 g/cm^3 for SPC/E water at 240 K[51]) suggests that both excess and defect with respect to tetrahedral coordination facilitate water mobility. This is not the case for water in the binary mixture for which the monotonic increase of mobility with the number of neighbors (see Figure 19) reflects the difference in mobility of water and glucose: The existence of more water neighbors provides more pathways for relaxation for water in an environment of low mobile glucose molecules.

The quantification of the effect of the facilitation on the heterogeneous dynamics of water requires the complementary evaluation of other sources of heterogeneity, such as the existence of "islands of mobility" in the overall mixture. These factors will be presented in a forthcoming publication.[52]

5. Conclusions

We studied the structure and translational dynamics of a binary mixture with components of different size and molecular complexity, although similar interactions. Our study of the translational dynamics in a supercooled 12.2 wt % water−glucose mixture reveals the existence of different mechanisms for the translational diffusion of these molecules. The sugar center of mass diffusion is continuous, whereas water mobility results from combining small step (continuous) and water size jumps. These mechanisms had been suggested from the analysis of neutron scattering of water−carbohydrate mixtures,[8,53] and this work presents a striking confirmation along with a quantitative characterization of the nonexponential behavior and characteristic times in the T range 310−365 K. For temperatures $T \leq 280$ K, we observe that water diffusion is controlled by activated hopping events, with water relaxation times exceeding 10 ns. We find an increasing separation of time scales between the glucose matrix and the glucose while approaching the glass transition: at 250 K the water molecules already move in a translationally frozen matrix. This time scale separation for water

and glucose diffusion is the precursor of the experimentally observed water diffusivity in glassy water−carbohydrate[2−4] and other binary organic mixtures of different sized molecules.[14]

We find that the locally heterogeneous structure of water plays a key role in water diffusivity, particularly in the deep supercooled regime where the matrix diffusivity is negligible. Here the pathways provided by the water−water connectivity facilitate the mobility of water molecules. Through this facilitation mechanism, the heterogeneous environments of water in the solution contribute to the nonexponential, dynamically heterogeneous character of the relaxation. The relaxation is more nonexponential at the lowest temperatures, where the facilitation effect of water connectivity is more important due to the freezing of the sugar matrix.

The mobility of water in supercooled carbohydrate mixtures was found to be correlated with processes that affect the stability of foods and cryopreserved products, such as the crystallization of ice[54] and glass collapse.[55] The maximum water concentration that can be incorporated into carbohydrate glasses is approximately 20 wt %, irrespective of the nature of the saccharide.[33,54,56−58] Cooling a solution with greater water content will lead to crystallization of the excess water as ice. This water concentration for water−glucose, 19 wt %, coincides with the formation of a percolated water network in the mixtures between 16 and 20 wt % Our results indicate that water percolation is independent of the composition of the saccharide mixture: we observed water percolation in the same range of water content for glucose (this work), sucrose,[11] a mixture of glucose, maltose, fructose and sucrose,[24] and a polydisperse mixture of maltooligosaccharides.[24] This shows that the knowledge of the water distribution and facilitation mechanisms in water−carbohydrate mixtures may provide invaluable help in the rationalization of the design of new products with extended shelf life.

References and Notes

(1) Levine, H.; Slade, L. *Cryo-Lett.* **1988**, *9*, 21.

(2) Tromp, R. H.; Parker, R.; Ring, S. G. *Carbohydr. Res.* **1997**, *303*, 199.

(3) Hills, B. P.; Wang, Y. L.; Tang, H. R. *Mol. Phys.* **2001**, *99*, 1679.

(4) van den Dries, I. J.; van Dusschoten, D.; Hemminga, M. A. *J. Phys. Chem. B* **1998**, *102*, 10483.

(5) Lievonen, S. M.; Roos, Y. H. *J. Food Sci.* **2002**, *67*, 2100.

(6) Le Meste, M.; Champion, D.; Roudaut, G.; Blond, G.; Simatos, D. *J. Food Sci.* **2002**, *67*, 2444.

(7) Magazu, S.; Maisano, G.; Majolino, D. *Prog. Theor. Phys. Suppl.* **1997**, 195.

(8) Feeney, M.; Brown, C.; Tsai, A.; Neumann, D.; Debenedetti, P. G. *J. Phys. Chem. B* **2001**, *105*, 7799.

(9) Moran, G. R.; Jeffrey, K. R. *J. Chem. Phys.* **1999**, *110*, 3472.

(10) Champion, D.; Hervet, H.; Blond, G.; LeMeste, M.; Simatos, D. *J. Phys. Chem. B* **1997**, *101*, 10674.

(11) Molinero, V.; Cagin, T.; Goddard, W. A., III. *Chem. Phys. Lett.* **2003**, *377*, 469.

(12) Noel, T. R.; Parker, R.; Ring, S. G. *Carbohydr. Res.* **1996**, *282*, 193.

(13) Roberts, C. J.; Debenedetti, P. G. *J. Phys. Chem. B* **1999**, *103*, 7308.

(14) Blochowicz, T.; Karle, C.; Kudlik, A.; Medick, P.; Roggatz, I.; Vogel, M.; Tschirwitz, C.; Wolber, J.; Senker, J.; Rossler, E. *J. Phys. Chem. B* **1999**, *103*, 4032.

(15) Allen, M. P.; Tildesley, D. J. *Computer simulation of liquids*; Clarendon Press and Oxford University Press: Oxford, England, and New York, 1989.

(16) Accelerys, M. S. I.-. Cerius2; 4.0 ed. San Diego, CA, 1999.

(17) Hoover, W. G. *Phys. Rev. A* **1985**, *31*, 1695.

(18) Parrinello, M.; Rahman, A. *J. Appl. Phys.* **1981**, *52*, 7182.

(19) Mayo, S. L.; Olafson, B. D.; Goddard, W. A. *J. Phys. Chem.* **1990**, *94*, 8897.

(20) Rappe, A. K.; Goddard, W. A. *J. Phys. Chem.* **1991**, *95*, 3358.

(21) Karasawa, N.; Goddard, W. A. *J. Phys. Chem.* **1989**, *93*, 7320.

(22) Molinero, V.; Goddard, W. A., III. M3B: a coarse grain model for the simulation of malto-oligosaccharides and their water mixtures. In *J. Phys. Chem. B* **2004**, *108*, 1414.

(23) Goldberg, R. N.; Tewari, Y. B. *J. Phys. Chem. Ref. Data* **1989**, *18*, 809.

(24) Molinero, V.; Goddard, W. A., III. Unpublished results. The crystal densities correspond to averages over 25 *NPT* MD of periodic cells with 32 β-fructose (II) and 24 α-glucose (IV), starting from the available X-ray structures. The study of the water percolation was performed following the same procedure described in this work on atomistic mixtures of glucose, fructose, maltose and sucrose with water content in the range 8−20 wt % at 343 K and coarse grain mixtures of malto-oligosaccharides with degree of polymerization 1−12 and water content 8−20 wt % at 330 K.

(25) Reiser, P.; Birch, G. G.; Mathlouthi, M. Physical Properties. In *Sucrose: Properties and Applications*; Mathlouthi, M. R. P., Ed.; Blackie Academic & Professional: Glasgow, Scotland, 1995; p 186.

(26) Hanson, J. C.; Sieker, L. C.; Jensen, L. H. *Acta Crystallogr., Sect. B: Struct. Sci.* **1973**, *B 29*, 797.

(27) Takagi, S.; Jeffrey, G. A. *Acta Crystallogr., Sect. B: Struct. Sci.* **1977**, *33*, 3510.

(28) Goddard, W. A.; Cagin, T.; Blanco, M.; Vaidehi, N.; Dasgupta, S.; Floriano, W.; Belmares, M.; Kua, J.; Zamanakos, G.; Kashihara, S.; Iotov, M.; Gao, G. H. *Comput. Theor. Polym. Sci.* **2001**, *11*, 329.

(29) Ekdawi-Sever, N. C.; Conrad, P. B.; de Pablo, J. J. *J. Phys. Chem. A* **2001**, *105*, 734.

(30) Louis, A. A. *J. Phys.: Condens. Matter* **2002**, *14*, 9187.

(31) Caffarena, E. R.; Grigera, J. R. *Carbohydr. Res.* **1997**, *300*, 51.

(32) Caffarena, E. R.; Grigera, J. R. *Carbohydr. Res.* **1999**, *315*, 63.

(33) Roos, Y. *Carbohydr. Res.* **1993**, *238*, 39.

(34) Kob, W.; Andersen, H. C. *Phys. Rev. E* **1995**, *51*, 4626.

(35) Magazu, S.; Villari, V.; Migliardo, P.; Maisano, G.; Telling, M. T. F. *J. Phys. Chem. B* **2001**, *105*, 1851.

(36) Hansen, J. P.; McDonald, I. R. *Theory of simple liquids*, 2nd ed.; Academic Press: London and Orlando, FL, 1986.

(37) Gallo, P.; Sciortino, F.; Tartaglia, P.; Chen, S. H. *Phys. Rev. Lett.* **1996**, *76*, 2730.

(38) Boon, J.-P.; Yip, S. *Molecular hydrodynamics*; McGraw-Hill: New York, 1980.

(39) Arbe, A.; Colmenero, J.; Monkenbusch, M.; Richter, D. *Phys. Rev. Lett.* **1998**, *81*, 590.

(40) Singwi, K. S.; Sjolander, A. *Phys. Rev.* **1960**, *119*, 863.

(41) Magazu, S.; Villari, V.; Migliardo, P.; Maisano, G.; Telling, M. T. F.; Middendorf, H. D. *Physica B* **2001**, *301*, 130.

(42) Teixeira, J.; Bellissentfunel, M. C.; Chen, S. H.; Dianoux, A. J. *Phys. Rev. A* **1985**, *31*, 1913.

(43) Lewis, L. J.; Wahnstrom, G. *Phys. Rev. E* **1994**, *50*, 3865.

(44) Giovambattista, N.; Starr, F. W.; Sciortino, F.; Buldyrev, S. V.; Stanley, H. E. *Phys. Rev. E* **2002**, *65*, art. no.

(45) Girlich, D.; Ludemann, H. D. *Z. Naturforsch. C−J. Biosci.* **1994**, *49*, 250.

(46) Chan, R. K.; Pathmanathan, K.; Johari, G. P. *J. Phys. Chem.* **1986**, *90*, 6358.

(47) Sastry, S.; Debenedetti, P. G.; Stillinger, F. H. *Nature (London)* **1998**, *393*, 554.

(48) Wahnstrom, G. *Phys. Rev. A* **1991**, *44*, 3752.

(49) Sciortino, F.; Geiger, A.; Stanley, H. E. *J. Chem. Phys.* **1992**, *96*, 3857.

(50) Sciortino, F.; Geiger, A.; Stanley, H. E. *Nature (London)* **1991**, *354*, 218.

(51) Netz, P. A.; Starr, F. W.; Barbosa, M. C.; Stanley, H. E. *Physica A* **2002**, *314*, 470.

(52) Molinero, V.; Goddard, W. A., III. Manuscript in preparation.

(53) Magazu, S.; Maisano, G.; Middendorf, H. D.; Migliardo, P.; Musolino, A. M.; Villari, V. *J. Phys. Chem. B* **1998**, *102*, 2060.

(54) Ablett, S.; Clarke, C. J.; Izzard, M. J.; Martin, D. R. *J. Sci. Food Agr.* **2002**, *82*, 1855.

(55) van den Dries, I. J.; Besseling, N. A. M.; van Dusschoten, D.; Hemminga, M. A.; van der Linden, E. *J. Phys. Chem. B* **2000**, *104*, 9260.

(56) Roos, Y.; Karel, M. *Cryo-Lett.* **1991**, *12*, 367.

(57) Roos, Y.; Karel, M. *J. Food Sci.*

(58) Ablett, S.; Izzard, M. J.; Lillford, P. J. *J. Chem. Soc., Faraday Trans.* **1992**, *88*, 789.